Biochemical Pharmacology, Vol. 60, pp. 55–65, 2000.

ELSEVIER

ISSN 0006-2952/00/$–see front matter
PII S0006-2952(00)00287-2

Kinetics and Mechanism of the Reaction of Aminoguanidine with the α-Oxoaldehydes Glyoxal, Methylglyoxal, and 3-Deoxyglucosone under Physiological Conditions

Paul J. Thornalley, Alexander Yurek-George and Ongian K. Argirov*

Department of Biological Sciences, University of Essex, Central Campus, Wivenhoe Park, Colchester CO4 3SQ, Essex, U.K.

ABSTRACT. Aminoguanidine (AG), a prototype agent for the preventive therapy of diabetic complications, reacts with the physiological α-oxoaldehydes glyoxal, methylglyoxal, and 3-deoxyglucosone (3-DG) to form 3-amino-1,2,4-triazine derivatives (T) and prevent glycation by these agents *in vitro* and *in vivo*. The reaction kinetics of these α-oxoaldehydes with AG under physiological conditions pH 7.4 and 37° was investigated. The rate of reaction of AG with glyoxal was first order with respect to both reactants; the rate constant $k_{AG,G}$ was $0.892 \pm 0.037\ M^{-1}\ sec^{-1}$. The kinetics of the reaction of AG with 3-DG were more complex: the rate equation was $d[T]_o/dt$ (initial rate of T formation) $= [3\text{-DG}](k_{AG,3\text{-DG}}[AG] + k_{3\text{-DG}})$, where $k_{AG,3\text{-DG}} = (3.23 \pm 0.25) \times 10^{-3}\ M^{-1}\ sec^{-1}$ and $k_{3\text{-DG}} = (1.73 \pm 0.08) \times 10^{-5}\ sec^{-1}$. The kinetics of the reaction of AG with methylglyoxal were consistent with the reaction of both unhydrated (MG) and monohydrate (MG-H_2O) forms. The rate equation was $d[T]_o/dt = \{k_1 k_{AG,MG}/(k_{-1} + k_{AG,MG}[AG]) + k_{AG,MG\text{-}H_2O}\}[MG\text{-}H_2O][AG]$, where the rate constant for the reaction of AG with MG, $k_{AG,MG}$, was $178 \pm 15\ M^{-1}\ sec^{-1}$ and for the reaction of AG with MG-H_2O, $k_{AG,MG\text{-}H_2O}$, was $0.102 \pm 0.001\ M^{-1}\ sec^{-1}$; k_1 and k_{-1} are the forward and reverse rate constants for methylglyoxal dehydration MG-$H_2O \rightleftharpoons$ MG. The kinetics of these reactions were not influenced by ionic strength, but the reaction of AG with glyoxal and with methylglyoxal under MG-H_2O dehydration rate-limited conditions increased with increasing phosphate buffer concentration. Kinetic modelling indicated that the rapid reaction of AG with the MG perturbed the MG/MG-H_2O equilibrium, and the ratio of the isomeric triazine products varied with initial reactant concentration. AG is kinetically competent to scavenge the α-oxoaldehydes studied and decrease related advanced glycated endproduct (AGE) formation *in vivo*. This effect is limited, however, by the rapid renal elimination of AG. Decreased AGE formation is implicated in the prevention of microvascular complications of diabetes by AG. BIOCHEM PHARMACOL **60**;1:55–65, 2000. © 2000 Elsevier Science Inc.

KEY WORDS. glycation; glyoxal; methylglyoxal; 3-deoxyglucosone; aminoguanidine; diabetic complications

AGEs† are stable end-stage adducts formed by the glycation of proteins, nucleotides, and phospholipids. They are formed in physiological systems by glycation reactions of glucose and physiological α-oxoaldehydes, particularly glyoxal, methylglyoxal, and 3-DG with amino and guanidino groups [1]. Lysine, arginine, and N-terminal residues of proteins, guanyl bases of nucleotides, and phosphatidylethanolamine and phosphatidylserine are sites of glycation *in vivo*. The formation of AGEs *in vivo* has been linked to the development of disease, the chronic clinical complications associated with diabetes mellitus (retinopathy, neuropathy, and nephropathy), cataract, macrovascular disease, kidney failure, and Alzheimer's disease [2–6]. Pharmacological intervention to scavenge these α,β-dicarbonyl compounds is likely to be an effective strategy to inhibit the formation of AGEs and prevent AGE-mediated processes linked to disease. A lead compound of this type, AG, also known as Pimagedine, is currently under clinical evaluation. AG reacts with glyoxal, methylglyoxal, 3-DG and α,β-dicarbonyl moieties of glycated proteins to form 3-amino-1,2,4-triazine derivatives [7–9] (Fig. 1). It may thereby prevent the formation of AGEs. Despite the demonstrable inhibition of AGE formation by AG *in vitro* and *in vivo* [7, 10, 11], where 3-amino-1,2,4-triazine derivatives derived from glyoxal (**I**), methylglyoxal (**II** and **III**), and 3-DG (**IV** and **V**) were recently detected [12], little quantitative

* Corresponding author: Professor Paul J. Thornalley, Glutathione–Glyoxalase–Glycation Research Group, Department of Biological Sciences, University of Essex, Central Campus, Wivenhoe Park, Colchester CO4 3SQ, Essex, U.K. Tel. 0044 1206 873010; FAX 0044 1206 873010; E-mail: thorp@essex.ac.uk

† *Abbreviations:* AG, aminoguanidine; AGE, advanced glycated endproduct; AGE-HSA, human serum albumin highly modified by glucose-derived AGE; 3-DG, 3-deoxyglucosone; MG, methylglyoxal, unhydrated form; MG-H_2O, methylglyoxal monohydrate; MG-$(H_2O)_2$, methylglyoxal dihydrate; MG_{Tot}, total methylglyoxal concentration; T, 3-amino-1,2,4-triazine derivative; 3,5-T, 3-amino-5-methyl-1,2,4-triazine; 3,6-T, 3-amino-6-methyl-1,2,4-triazine; and $d[T]_o/dt$, initial rate of 3-amino-1,2,4-triazine derivative formation.

Received 2 September 1999; accepted 10 December 1999.

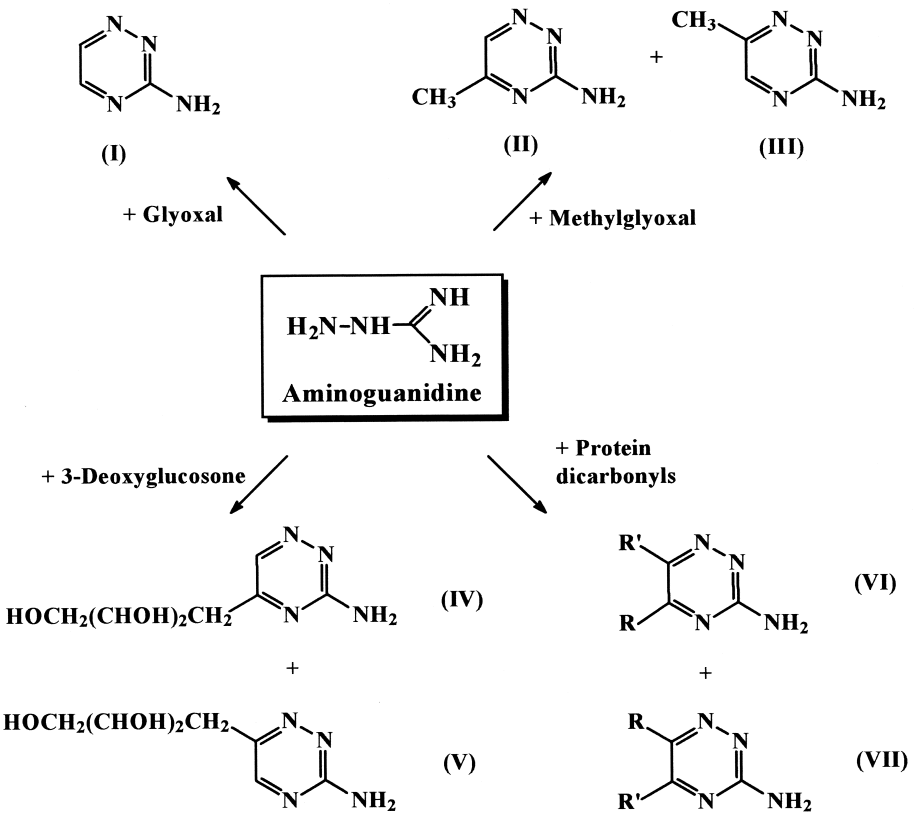

FIG. 1. The reaction of AG with glyoxal, methylglyoxal, 3-deoxyglucosone, and α,β-dicarbonyl compounds.

kinetic data on the reactivity of AG with these α-oxoaldehydes are available. Moreover, we suspected that the kinetics of the reaction of methylglyoxal with AG were more complex than initially reported [7] because of the unexpected formation of the two isomeric triazine products, 3,5-T (**II**) and 3,6-T (**III**), in approximately equal amounts (see below).

We present herein a study of the kinetics of reaction of glyoxal, methylglyoxal, and 3-DG under physiological conditions and associated kinetic modelling of 3,5-T and 3,6-T formation from the reaction of AG with methylglyoxal.

MATERIALS AND METHODS

Materials

Glyoxal (40% aqueous solution), AG hydrochloride, and 3-amino-1,2,4-triazine were purchased from Sigma. Methylglyoxal was prepared by acid hydrolysis of methylglyoxal dimethyl acetal, purified by fractional distillation under reduced pressure as described previously [13]. 3-DG was prepared and purified as described [14].

3-Amino-1,2,4-triazine derivatives were prepared by incubating glyoxal, methylglyoxal, and 3-DG (20 mM) with 20 mM AG hydrochloride in 50 mM sodium phosphate buffer in D_2O, pD 7.4 and 37°, until the reaction had gone to >90% of completion. ^1H NMR (270 MHz; D_2O, with chemical shift standard 3-(trimethylsilyl)-1-propane sulphonic acid, sodium salt DSS) gave chemical shift δ_H (ppm) and coupling constant $J_{x,y}$ (Hz) values as follows. 3-Amino-1,2,4-triazine: 8.36 (1H, d, $J_{5,6}$ 2.0, 5-H), 8.59 (1H, d, $J_{5,6}$ 2.0, 6-H); 3,5-T (41%): 2.41 (3H, s, 5-Me), 8.50 (1H, s, 5-H); and 3,6-T (59%) 8.31 (1H, s, 5-H), 2.46 (3H, s, 6-Me). 3-Amino-5-(2,3,4-trihydroxybutyl)-1,2,4-triazine (42%): 8.54 (1H, s, 6-H), 4.04 (1H, m, $J_{1A',1B'}$ − 6.0, H-$1'_A$), 3.91 (1H, m, $J_{1A',1B'}$ − 6.0, H-$1'_A$), 3.66 (1H, m, H-2′), 3.79 (1H, dd, $J_{3',4A'}$ 6.8, $J_{3',4B'}$ 4.0, H-3′), 3.67 (1H, dd, $J_{4A',4B'}$ − 6.4, $J_{3',3B'}$ 2.4, H-$4'_B$), 3.61 (1H, dd, − $J_{4A',4B'}$ 6.4, $J_{4A',3'}$ 4.4, H-$4'_A$); and 3-amino-6-(2,3,4-trihydroxybutyl)-1,2,4-triazine (58%): 8.33 (1H, s, 5-H), 4.04 (1H, m, $J_{1A',1B'}$ − 6.0, H-$1'_B$), 3.91 (1H, m, $J_{1A',1B'}$ − 6.0, H-$1'_A$), 3.66 (1H, m, H-2′), 3.79 (1H, dd, $J_{3',4A'}$ 6.8, $J_{3',4B'}$ 4.0, H-3′), 3.67 (1H, dd, $J_{4A',4B'}$ − 6.4, $J_{3',3B'}$ 2.4, H-$4'_B$), 3.61 (1H, dd, $J_{4A',4B'}$ − 6.4, $J_{4A',3'}$ 4.4, H-$4'_A$). The percentages of triazine isomer formed were deduced from measurement of the 5 and 6 proton integrals in the ^1H NMR spectra.

Kinetics of the Scavenging of Physiological α-Oxoaldehydes by AG

The reaction of glyoxal with AG in 50 mM sodium phosphate buffer, pH 7.4 and 37°, was followed by monitoring the absorbance of the triazine product, 3-amino-1,2,4-triazine, at 320 nm; the extinction coefficient ϵ_{320} = 2319 ± 27 M^{-1} cm^{-1} (slit width = 1, N = 20). Initial rate

measurements were made at constant initial glyoxal concentration (0.05, 0.10, 0.20, 0.50, and 1.00 mM) with 0.1–1.5 mM AG (Fig. 3a), and constant initial AG concentration (0.10, 0.20, 0.35, 0.50, 1.00, and 1.50 mM) with 0.05–1.00 mM glyoxal (Fig. 3b) in quadruplicate. The reaction of 3-DG with AG in 50 mM sodium phosphate buffer pH 7.4 and 37° was followed by monitoring the absorbance of the triazine products (3-amino-5-(2,3,4-trihydroxybutyl)-1,2,4-triazine and 3-amino-6-(2,3,4-trihydroxybutyl)-1,2,4-triazine combined) at 317 nm; the extinction coefficients ϵ_{317} were 3360 M^{-1} cm^{-1} and 3130 M^{-1} cm^{-1}, respectively [8]. Initial rate measurements were made at constant initial 3-DG concentration (0.50, 1.00, 1.50, 2.00, and 2.50 mM) with 2–20 mM AG (Fig. 3c), and constant initial AG concentration (2, 5, 10, 15, and 20 mM) with 0.5–2.50 mM 3-DG (Fig. 3d). The reaction of methylglyoxal with AG in 50 mM sodium phosphate buffer pH 7.4 and 37° was followed by monitoring the absorbance of the triazine products (3-amino-5-methyl-1,2,4-triazine and 3-amino-6-methyl-1,2,4-triazine combined) at 320 nm. The extinction coefficients of the isomeric triazines were not significantly different: the mean extinction coefficient for 5-/6-methyl-3-amino-1,2,4-triazine ϵ_{320} in 50 mM sodium phosphate, pH 7.4 and 37°, was 2411 ± 9 M^{-1} cm^{-1} [7]. Initial rate measurements were made at constant initial methylglyoxal concentration (0.05, 0.10, 0.20, 0.50, and 1.00 mM) with 0.05–3.50 mM AG (Fig. 3e), and constant initial AG concentration (0.10, 0.20, 0.35, 0.50, 1.00, 1.50, 2.00, 2.50, 3.00, and 3.50 mM) with 0.05–1.00 mM methylglyoxal (Fig. 3f) in quadruplicate. This is the total methylglyoxal concentration [MG_{Tot}] where [MG_{Tot}] = [MG] + [MG-H_2O] + [MG-$(H_2O)_2$]. The effect of the ionic strength on the rate of reaction of AG with the α-oxoaldehydes was studied in the ionic strength range 111–222 mM, and the effect of phosphate buffer concentration (10–100 mM) was investigated.

Kinetic Modelling

Kinetic modelling was performed for the reaction of 1.0 mM methylglyoxal with 0.2–1.0 mM AG in 200-μM increments. The ratio of the two triazine isomers formed at end point for equimolar AG with methylglyoxal was modelled in the range of 100 μM to 100 mM reactants. The rate expressions deduced for the reaction of α-oxoaldehydes with AG were used to deduce initial rates of reaction of 100 nM α-oxoaldehyde with 10–50 μM AG.

Data Analysis

Linear regression and non-linear regression were performed using the ENZFITTER program (Biosoft). Kinetic modelling was performed using the Gepasi 3 kinetic program [15].

RESULTS

Spectrophotometric Study of the Formation of 3-Amino-1,2,4-triazine Derivatives by the Reaction of AG with α-Oxoaldehydes

When glyoxal, methylglyoxal, and 3-DG reacted with AG in 50 mM sodium phosphate buffer, pH 7.4 and 37°, there was a increase in UV absorbance at *ca.* 225 and 320 nm. This was characteristic of the formation of the 3-amino-1,2,4-triazine products [7, 8]. The rate of reaction was much slower with 3-DG compared to that of glyoxal and methylglyoxal. To view the reaction progress, therefore, UV spectra were recorded at 1800-sec (30-min) intervals over 21,600 sec (6 hr) for 50 μM α-oxoaldehyde with 200 μM AG (for glyoxal and methylglyoxal) and 20 mM AG (for 3-DG) (Fig. 2). The 100-fold increase in AG in the reaction of 3-DG still did not increase the rate of reaction sufficiently to take it to completion in the time period studied.

The triazine products of the reaction of glyoxal, methylglyoxal, and 3-DG with AG were also analysed by ^1H NMR spectroscopy. The characteristics of the triazine products were similar to those reported previously [7, 8, 16]. For the methylglyoxal reaction, the ratio of the 5-/6-methyl isomers was 41:59, and for the 3-DG reaction, the ratio of the 5-/6-(2,3,4-trihydroxybutyl) isomers was 42:58. No evidence of formation of bis(guanylhydrazone) adducts was found. The formation of these predominates at low pH [17] (data not shown).

Reaction Kinetics of the Scavenging of Glyoxal, Methylglyoxal, and 3-DG by AG under Physiological Concentrations

The rate of the reaction of glyoxal with AG under physiological conditions, pH 7.4 and 37°, determined as the initial rate of formation of 3-amino-1,2,4-triazine, $d[T]_o/dt$, was first order with respect to glyoxal and AG (Fig. 3, a and b). The plot of $d[T]_o/dt$ against initial glyoxal concentration curved slightly at 0.2–1.0 mM glyoxal, suggesting that extrapolation to higher glyoxal concentrations than studied herein would approach a limiting value of $d[T]_o/dt$. The rate expression was $d[T]_o/dt = k_{AG,G}$ [Glyoxal][AG], where the rate constant $k_{AG,G}$ = 0.892 ± 0.037 M^{-1} sec^{-1} (N = 11). The rate of reaction was not affected by ionic strength. It was increased, however, by increasing the concentration of phosphate buffer. Regression of the rate V ($Msec^{-1}$) on phosphate buffer concentration [Phosphate] (M), normalised to the extrapolated rate at zero phosphate concentration $V_{P,0}$, gave: $V = V_{P,0}$ {1 + (6.6 ± 0.2) × [Phosphate]}; ($r = 0.97$, $P < 0.001$, N = 20) (data not shown). The value of $k_{AG,G}$ for physiological phosphate concentration (4 mM, in blood plasma) was 0.688 ± 0.029 M^{-1} sec^{-1}.

The rate of reaction of 3-DG with AG under physiological conditions, pH 7.4 and 37°, was first order with respect to 3-DG and had kinetic components first and zeroth order with respect to AG (Fig. 3, c and d). The rate expression

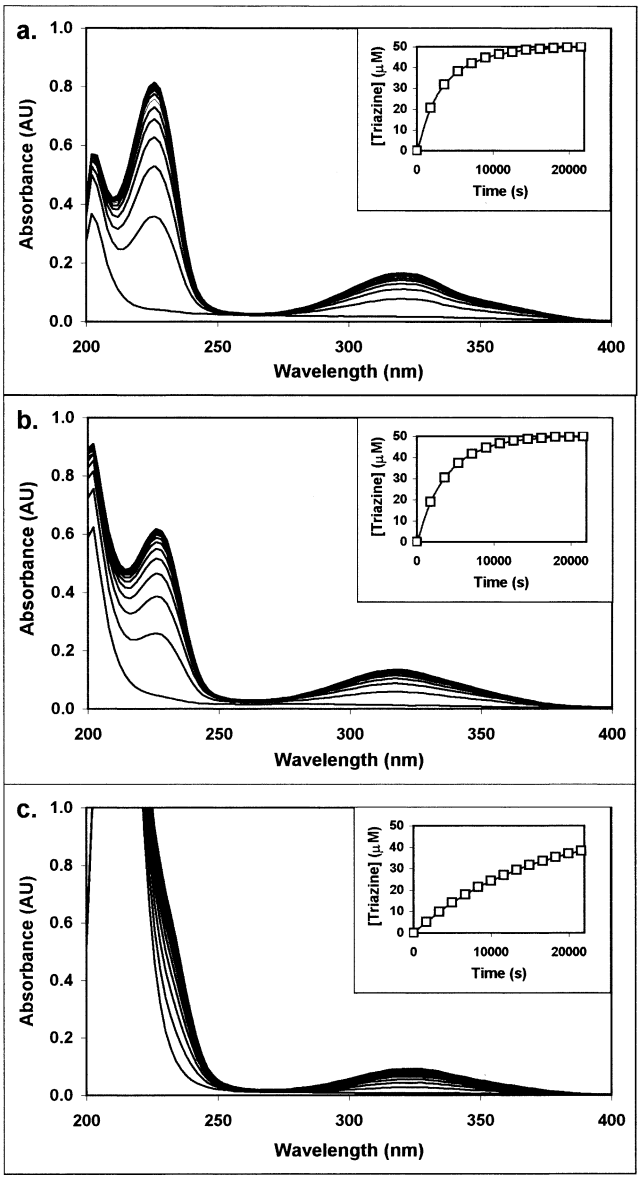

FIG. 2. Spectrophotometric study of the reaction of α-oxoaldehydes with AG. Key: (a) glyoxal; (b) methylglyoxal; (c) 3-DG. In the inset is given the concentration time–course of the triazine product formation. α-Oxoaldehyde (50 μM) was incubated with 200 μM AG (except 20 mM AG for 3-DG) in 50 mM sodium phosphate buffer, pH 7.4 and 37°. UV absorbance spectra were recorded at 30-min intervals over 6 hr. AU, absorbance units.

was $d[T]_o/dt = [3\text{-DG}](k_{AG,3\text{-DG}}[AG] + k_{3\text{-DG}})$, where the rate constant values were $k_{AG,DG} = (3.23 \pm 0.25) \times 10^{-3}$ M^{-1} sec^{-1} and $k_{3\text{-DG}} = (1.73 \pm 0.08) \times 10^{-5}$ sec^{-1} (N = 11). The rate was not affected by ionic strength nor by phosphate buffer concentration.

The reaction of methylglyoxal with AG was first order with respect to $[MG]_{Tot}$, but first order with respect to AG only at low AG concentration, approaching zeroth order at high AG concentration (Fig. 3, e and f). This could be explained by routes of triazine formation: one from MG and one from MG-H_2O. The kinetic model for this is:

$$\text{MG-H}_2\text{O} \underset{k_{-1}}{\overset{k_1}{\rightleftharpoons}} \text{MG} \xrightarrow{k_{AG,MG}[AG]} \text{Triazine}$$

$$\downarrow k_{AG,MG\text{-}H_2O}[AG]$$

Triazine

The rate of the reaction was determined as the rate of triazine formation d[T]/dt. Assuming the principle of stationary states for MG, it can be shown that $d[T]/dt = \{k_1 k_{AG,MG}/(k_{-1} + k_{AG,MG}[AG]) + k_{AG,MG\text{-}H_2O}\}[MG\text{-}H_2O][AG]$. When $k_{-1} \ll k_{AG,MG}[AG]$, that is at low concentrations of AG, $d[T]/dt \approx (k_1 k_{AG,MG}/k_{-1} + k_{AG,MG\text{-}H_2O})[MG\text{-}H_2O][AG]$. When $k_{-1} \ll k_{AG,MG}[AG]$, i.e. at high AG concentrations, $d[T]/dt = (k_1 + k_{AG,MG\text{-}H_2O}[AG])[MG\text{-}H_2O]$. We assume here that MG-H_2O remains in equilibrium with MG-$(H_2O)_2$ where $K_{MG\text{-}(H_2O)_2/MG\text{-}H_2O} = [MG - H_2O]/[MG - (H_2O)_2] = 2.41$ [18]. Under initial rate conditions at constant $[MG_{Tot}]_o$ and high varying $[AG]_o$, the slope of the plot of $d[T]_o/dt$ versus $[AG]_o$ is $m_{highAG} = k_{AG,MG\text{-}H_2O}[MG\text{-}H_2O]_o$. Knowing $[MG\text{-}H_2O]_o$, the value of $k_{AG,MG\text{-}H_2O}$, the rate constant for the reaction of AG with MG-H_2O was therefore determined: $k_{AG,MG\text{-}H_2O} = 0.102 \pm 0.001$ M^{-1} sec^{-1} (N = 5). The $k_{AG,MG\text{-}H_2O}[AG][MG\text{-}H_2O]$ component of the observed initial rates was then subtracted such that $(d[T]/dt)_{o,corrected} = k_1[MG\text{-}H_2O]$. Hence, the rate constant for the dehydration of MG-H_2O, k_1, was determined: $k_1 = (7.98 \pm 0.12) \times 10^{-4}$ sec^{-1} (N = 5). The equilibrium constant for the MG-H_2O/MG equilibrium was taken from the literature, $K_{MG\text{-}H_2O,MG} = 0.019$ [19], and the rate constant for the hydration of MG was deduced: $k_{-1} = 0.042 \pm 0.001$ sec^{-1}. These values were then used to fit initial rate data at constant $[MG\text{-}H_2O]_o$, varying $[AG]_o$, by non-linear regression to solve for the rate constant for the reaction of AG with MG, $k_{AG,MG,} = 178 \pm 15$ M^{-1} sec^{-1} (N = 5). The overall rate constant for the reaction of AG with methylglyoxal (unhydrated and monohydrate forms at equilibrium), $k_{AG,MG_{Tot}}$, was 2.58 ± 0.17 M^{-1} sec^{-1} (N = 5). There was increased deviation of the experimental data from the kinetic model with increase of methylglyoxal concentration.

The rate of reaction of methylglyoxal with AG was not affected by change in ionic strength nor by phosphate buffer under conditions where the dehydration of methylglyoxal was not rate-limiting. When the dehydration of methylglyoxal was rate-limiting, however, the rate of reaction increased significantly with increasing phosphate buffer concentration. Regression of the rate V ($Msec^{-1}$) on phosphate buffer concentration [Phosphate] (M), normalised to the extrapolated rate at zero phosphate concentration $V_{P,0}$, gave: $V = V_{P,0}\{1 + (4.0 \pm 0.3) \times [Phosphate]\}$; ($r = 0.948$, $P < 0.001$, N = 20) (data not shown).

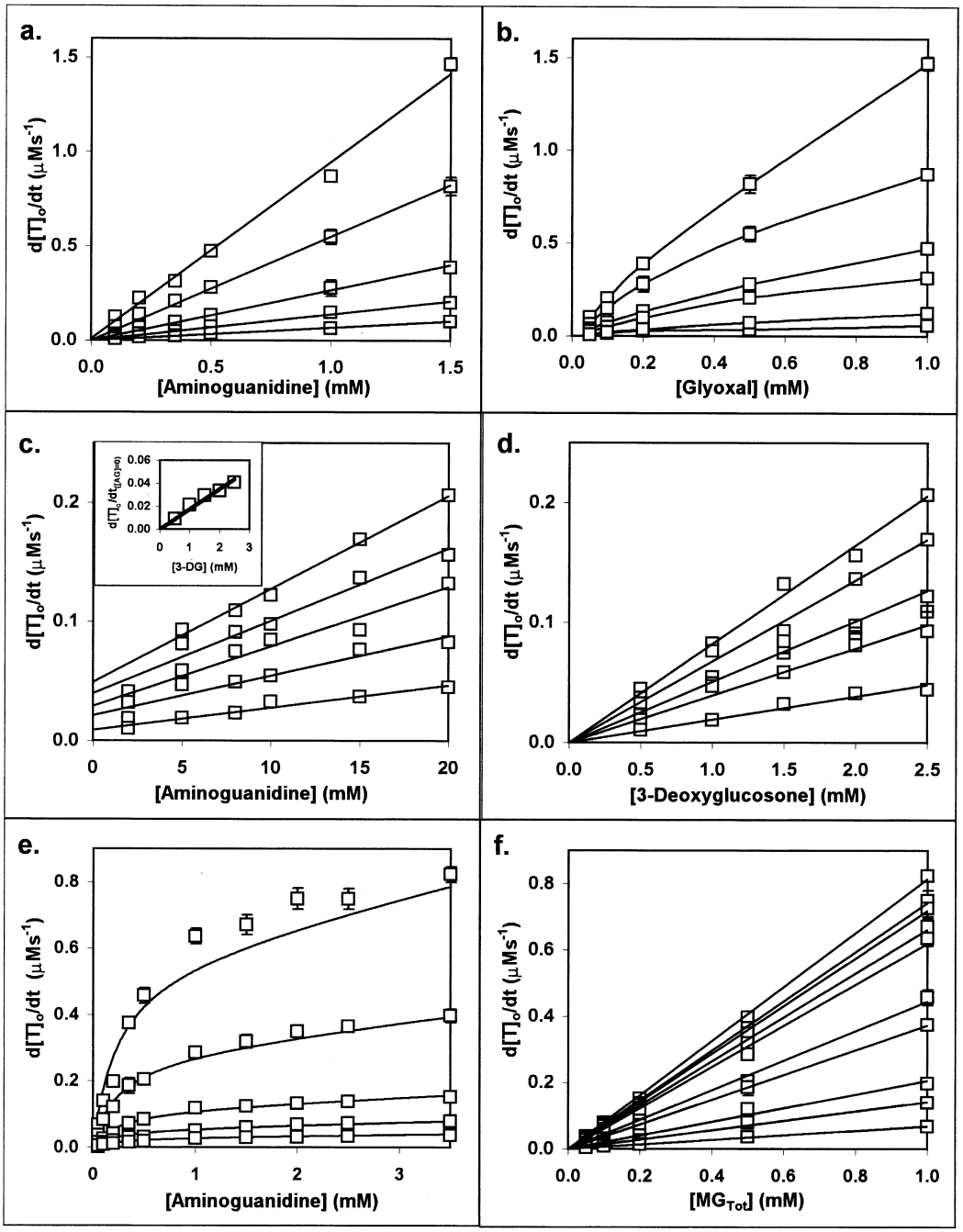

FIG. 3. Initial rate study of the reaction of α-oxoaldehydes with AG. Key: reaction with glyoxal (a and b), methylglyoxal (c and d), and 3-DG (e and f). The initial rate of triazine product formation $d[T]_o/dt$ was determined for constant [α-oxoaldehyde] with varying [AG] (left panels) and vice versa (right panels). Inset in (c) is the dependence of the intercept at [AG] = 0 on 3-DG concentration. Conditions are given in the Methods section. Data were fitted to linear regression equations except in (b), where data points were joined by linear interpolation, and in (e), where data were fitted to the equation $d[T]_o/dt = \{k_1 k_{AG,MG}/(k_{-1} + k_{AG,MG}[AG]) + k_{AG,MG\text{-}H_2O}\}[MG\text{-}H_2O][AG]$ solving for $k_{AG,MG}$. Data for a, b, e, and f are means ± SD (N = 4).

DISCUSSION

The kinetics of the reaction of α-oxoaldehydes with AG are complicated by interaction with unhydrated, monohydrate, and (where applicable) hemiacetal forms of the α-oxoaldehyde (Fig. 4). The hydrazino group of AG is the most reactive group of AG with α-oxoaldehydes. The interaction of the hydrazino group with the free aldehyde form of α-oxoaldehydes forms an initial aldimino adduct (Fig. 4, **VIIIa** and **VIIIb**) that cyclises to form the 5-alkyl-substituted 3-amino-1,2,4-triazine derivative. The interaction of the hydrazino group with the monohydrate and/or hemiacetal of α-oxoaldehydes forms an initial ketimino adduct (Fig. 4, **IXa** and **IXb**) that cyclises to form the 6-alkyl-substituted 3-amino-1,2,4-triazine derivative. The

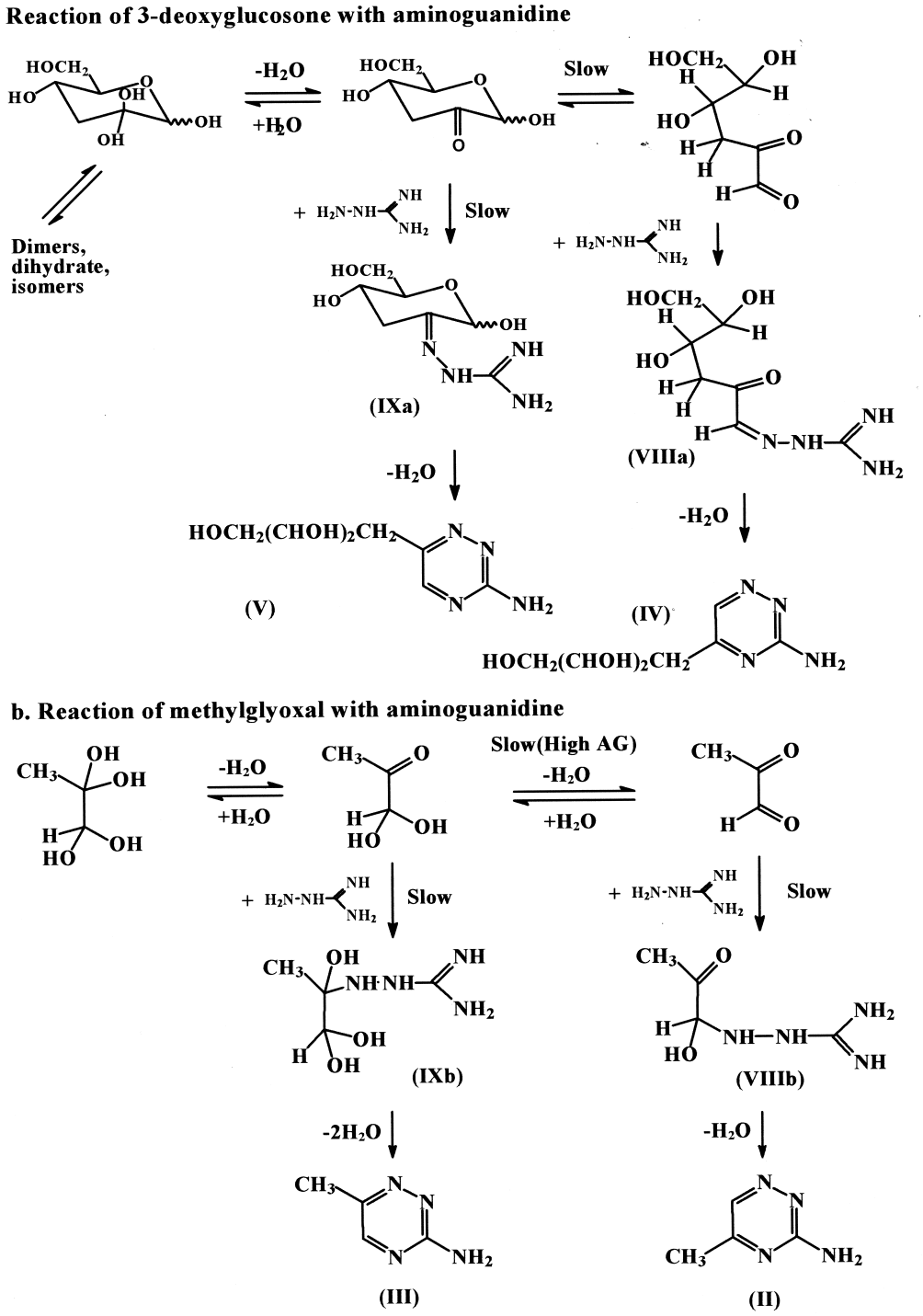

FIG. 4. Mechanistic interpretation of the kinetics of reaction of AG with (a) 3-deoxyglucosone and (b) methylglyoxal.

observed reaction kinetics are, therefore, the sum of rate-limiting steps of these two reaction pathways (except for glyoxal where there is no keto group).

Glyoxal reacted with AG to form 3-amino-1,2,4-triazine (**I**). Glyoxal is highly hydrated in aqueous solution: in the range of concentrations studied herein, glyoxal exists as *ca.* 0.005% unhydrated form, *ca.* 0.5% monohydrate, *ca.* 1–2% as dimers, and the remainder dihydrate [20, 21]. The deviation of $d[T]_o/dt$ from first-order kinetics at 0.2–1.0 mM glyoxal may be due to the dimerisation of glyoxal. The rate of formation of 3-amino-1,2,4-triazine was also dependent on phosphate concentration. This may be due to catalysis of the dehydration of the glycosylamine glyoxal–AG adduct HCO-CH(OH)-NH-NH-C(=NH)NH_2, the putative initial mechanistic intermediate, by phosphate dianion HPO_4^{2-}.

The kinetics of the reaction of 3-DG with AG had a kinetic component that was independent of AG concen-

tration. This may be due to slow, rate-limiting ring opening of the cyclic hemiacetal of 3-DG followed by the rapid reaction of the hydrazino group of AG with the aldehyde group of acyclic 3-DG. On dehydration and cyclisation, this forms 3-amino-5-(2,3,4-trihydroxybutyl)-1,2,4-triazine (**IV**). The second-order kinetic component may be due to the reaction of AG with the cyclic hemiacetal where interaction of the hydrazino group of AG with the keto group of cyclic 3-DG is rate-limiting. On dehydration and cyclisation, this forms 3-amino-6-(2,3,4-trihydroxybutyl)-1,2,4-triazine (**V**) (Fig. 4a). This accounts for the formation of two isomeric 3-amino-1,2,4-triazine products. 3-DG exists in many cyclic forms in aqueous solution: there are 5 major and at least 6 minor forms [22]. As expected, all NMR resonances of 3-DG were lost when the reaction with AG had gone to completion, being replaced by the NMR spectra of the 5-/6-(2,3,4-trihydroxybutyl)-3-amino-1,2,4-triazine products [8]. From the above analysis, the rate constant $k_{3\text{-DG}}$ may be equivalent to the rate of acyclisation of the hemiacetal of 3-DG. Indeed, a similar kinetic analysis was found for the reaction of 3-DG with thiol-containing nucleophiles, which gave a unimolecular kinetic component with a similar first-order rate constant value [23].

The kinetics of the reaction of methylglyoxal with AG were complex. Despite the previous fit of triazine concentration/time–course data for the reaction of 180 μM methylglyoxal to 1 mM AG to an integrated second-order rate equation [7], the initial rate of reaction did not increase proportionately with increased AG concentration at high AG concentrations (Fig. 3e). Moreover, under preparative conditions, methylglyoxal and AG unexpectedly formed the two triazine isomers, 3,5-T (**II**) and 3,6-T (**III**), in the ratio of *ca.* 1:1. Methylglyoxal exists in aqueous solution in three major forms: MG, MG-H_2O, and MG-$(H_2O)_2$. These forms are in dynamic equilibrium in the approximate ratio of 1:71:28. MG is more reactive than MG-H_2O, but the latter is present at much higher equilibrium concentration (Fig. 4b). As a consequence of the high reactivity of AG with MG, the prior dehydration of MG-H_2O to MG becomes rate-limiting at high AG concentration, and there is a kinetic component zeroth order with respect to AG in the overall reaction kinetics. Under these conditions, the rate increased with increasing concentration of phosphate buffer. This may be due to catalysis of the dehydration of MG-H_2O by phosphate dianion HPO_4^{2-}.

Given the complexity of the kinetics of the reaction of methylglyoxal with AG, the reaction kinetics were modelled, including the prediction of discrete formation of the isomeric triazine products. Time–course changes in the concentrations of MG, MG-H_2O, MG-$(H_2O)_2$, AG, 3,5-T, and 3,6-T are given for the reaction of 1.0 mM methylglyoxal with 0.2–1.0 mM AG in 0.2-mM concentration steps (Fig. 5). The initial concentration of MG was 0.013 mM. MG reacts rapidly with AG and the concentration of MG falls within the initial 30 sec (Fig. 5a, inset). In reaction models with residual methylglyoxal, the methylglyoxal hydration equilibria re-adjust to increase the concentration of MG from a minimum value in the initial 3000–6000 sec (Fig. 5a). The concentration of AG decreases rapidly in all reaction models (Fig. 5b). The concentrations of MG-H_2O and MG-$(H_2O)_2$ decreased proportionately during the reaction progress (Fig. 5, c and d), and the triazine 3,5-T was formed in *ca.* 9-fold excess over 3,6-T (Fig. 5, e and f). The formation of 3,5-T and 3,6-T at completion of the reaction of equimolar methylglyoxal and AG, scanning over reactant concentration, is given in Fig. 6f, inset. Only at 20 mM methylglyoxal and AG was the ratio of 3,5-T to 3,6-T concentrations *ca.* 1:1. These are the conditions employed in the preparative reaction for ^1H NMR spectroscopy described herein and in our previous study [7]. This model, therefore, predicted the experimental triazine isomer ratio. A similar kinetic model could not be constructed for the reaction of 3-DG with AG because of lack of kinetic constants on the hydration, cyclisation, and dimerisation of the α-oxoaldehyde.

The experimental initial rate data for the reaction of methylglyoxal with AG fitted the kinetic model except that deviations (i.e. initial rates higher than expected) were observed at high MG_{Tot} and AG concentrations. The kinetic analysis assumed the principle of stationary states for [MG], which assumes that d[MG]/dt = 0. From the kinetic modelling of the reaction of methylglyoxal with AG, it was predicted that [MG] changes, and this change is marked (>50%) for high AG concentration (Fig. 5a). The divergence of experimental data from the model at high MG_{Tot} and AG concentrations may be due to deviation from the principle of stationary states assumption under these conditions. Nevertheless, this did provide a model with reasonable fit to experimental data under other MG_{Tot} and AG concentration conditions.

The high reactivity of MG is of interest, since methylglyoxal formed from the degradation of triosephosphates and glycation reactions *in vivo* is expected to be formed as MG. Comparison of the relative rates of reaction of MG with water to form MG-H_2O, with AG to form triazines, and with cysteinyl residues to form the hemithioacetal in blood plasma can now be made. The respective rate constants are: k_{-1} = 0.042 sec^{-1}, $k_{AG,MG}$ 178 M^{-1} sec^{-1} (this work), and $k_{MG,CYS} = 4.1 \times 10^4$ M^{-1} sec^{-1} [24]; the concentration of cysteinyl thiols in plasma is *ca.* 500 μM, and a pharmacologically relevant concentration of AG is *ca.* 50 μM [25]. The relative rates of reaction of MG with water, AG, and cysteinyl thiols is *ca.* 1:0.21:488. When formed, therefore, MG will react rapidly with cysteine thiols of proteins and glutathione. Most methylglyoxal is detoxified by enzymatic conversion of the glutathione adduct to D-lactate by the glyoxalase system [26]. AG (50 μM) will not compete effectively with water for MG formed upon fragmentation of the hemithioacetal. Some studies have used much higher concentrations of AG (1–100 mM) [27, 28]. In these works, the 'nascent' MG may have been preferentially scavenged by AG. The high reactivity of α-oxoaldehydes when generated as unhydrated forms *in*

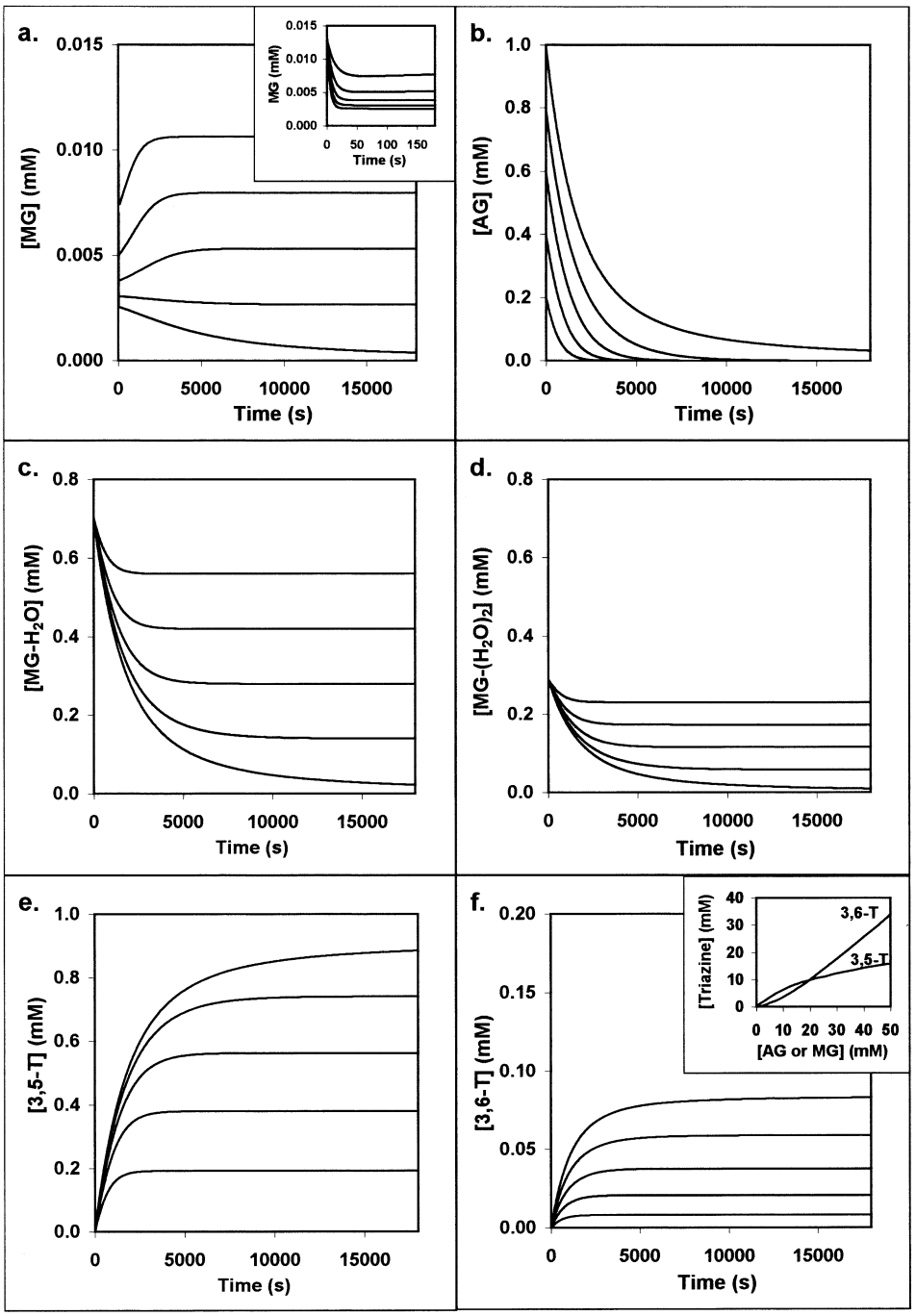

FIG. 5. Kinetic modelling of the reaction of methylglyoxal (1 mM) with 0.2–1.0 mM AG in 0.2-mM increments. Key: (a) MG, inset is a time-scale expansion of the initial 3 min of reaction; (b) AG; (c) MG-H_2O; (d) MG-$(H_2O)_2$; (e) 3,5-T; and (f) 3,6-T, inset is the concentrations of 3,5-T and 3,6-T at reaction completion from equimolar mixtures of reactants as a function of reactant concentration.

situ, "nascent α-oxoaldehydes," was noted in the inactivation of aldolase by hydroxypyruvaldehyde [29]. Similar arguments apply to the formation of glyoxal and 3-DG.

It would be instructive to model the kinetics of the scavenging of α-oxoaldehydes by AG at physiologically and pharmacologically relevant concentrations. A typical estimate of the concentration of glyoxal, methylglyoxal, and 3-DG in blood plasma of normal healthy human subjects is *ca.* 100 nM. This is increased 1- to 2-fold in diabetic subjects [30, 31]. A pharmacologically relevant range of AG concentration is 10–50 μM [25]. The rates of reaction of 10–50 μM AG with 100 nM glyoxal, methylglyoxal, and 3-DG were computed from the rate expressions given above (Fig. 6): this involves extrapolation to lower concentrations of α-oxoaldehydes than used in this study. The rate of reaction of AG with glyoxal and methylglyoxal increased

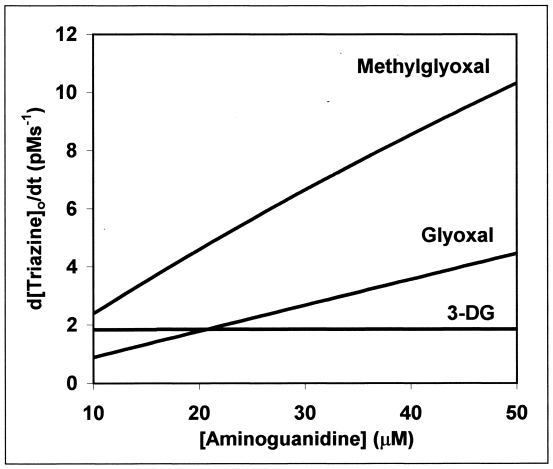

FIG. 6. Predicted rates of reaction of 10–50 μM AG with 100 nM α-oxoaldehyde under physiological conditions.

proportionately with AG concentration, whereas the rate of reaction of AG with 3-DG did not because the [AG]-independent kinetic pathway dominated under these conditions. It is likely, however, that as the AG concentration decreases, this reaction pathway will also become first order with respect to AG. Under physiological conditions, the reaction of methylglyoxal with AG proceeds mainly (96%) via the reaction pathway: MG + AG → 3,6-T.

AG also reacts with α,β-dicarbonyl compounds formed from the degradation of fructosamines in glucose-modified proteins [9]. In a recent study, we determined the concentration of α,β-dicarbonyls in AGE-modified proteins prepared *in vitro* by studying the reaction of [^{14}C]AG with AGE-HSA [32]. From the initial rate of binding of [^{14}C]AG to AGE-HSA and the concentration of α,β-dicarbonyls in AGE-HSA (determined from the extent of modification of AGE-HSA by [^{14}C]AG at end point), an estimate of the rate constant for the reaction of AG with α,β-dicarbonyl compounds in glycated proteins, $k_{AG,\alpha,\beta\text{-dicarbonyls}}$, was obtained: $k_{AG,\alpha,\beta\text{-dicarbonyls}} \approx 1.0 \pm 0.1\ M^{-1}\ sec^{-1}$ (N = 4). This is similar to the overall rate constants for the reaction of glyoxal and methylglyoxal with AG. An estimate of α,β-dicarbonyl concentration in plasma protein *in vivo* was *ca.* 0.5–1.0 μM [32]. It is expected, therefore, that AG reacts with α,β-dicarbonyl compounds of glycated proteins and α-oxoaldehydes at similar rates *in vivo*, and scavenging of both may be involved in its mechanism of action (Fig. 1). Recent analysis of AG adducts in the plasma of normal, healthy control and diabetic rats found the triazine adducts of methylglyoxal and 3-DG. The concentrations of the triazine adducts were increased *ca.* 10-fold in streptozotocin-induced diabetic rats [12]. We have attempted to model the *in vivo* effect of aminoguanidine on the plasma concentrations of glyoxal and methylglyoxal and the concentration of associated AGEs, using best estimates of fluxes of formation and glyoxalase system-dependent detoxification of these α-oxoaldehydes, and a plasma half-life of AG of 1.4 hr [25, 26, 33–35]. The models predict that AG decreases plasma α-oxoaldehyde concentrations and corresponding AGE formation, but levels remain above those of the normal healthy control. This effect rapidly decreases as AG is excreted, mostly (>95%) in the unmodified form (data not shown).

Glyoxal, methylglyoxal, and 3-DG are important physiological α-oxoaldehydes involved in the formation of AGEs. Glyoxal is formed by the degradation of glucose, glucose-modified proteins, and lipid peroxidation. Methylglyoxal is formed mainly by the fragmentation of triosephosphates, but also by the catabolism of ketone bodies and threonine and the degradation of glucose-modified proteins. 3-DG is formed by the fragmentation of fructose-3-phosphate and the degradation of glucose-modified proteins (reviewed in Ref. [1]). By intercepting these and other α,β-dicarbonyl metabolites, AG may delay the development of AGE-related pathogenesis. AG was also a potent reversible inhibitor of inducible nitric oxide synthase; the k_i value was *ca.* 10 μM [36]. It was also found to react with malondialdehyde, but from the published data [37] (assuming first-order dependency of AG and malondialdehyde), the rate constant value deduced is *ca.* 5000 times lower than that for the reaction with glyoxal, methylglyoxal, and α,β-dicarbonyl compounds. AG was found to have antioxidant activity and to inhibit hydrogen peroxide-induced apoptosis [38]. AG scavenges α-oxoaldehydes and may thereby prevent α-oxoaldehyde-induced apoptosis and associated oxidative stress [39, 40].

AG slowed the progression of retinopathy, neuropathy and nephropathy in streptozotocin-induced diabetic rats [10, 11, 41–44], but had no effect on the increased levels of glycated haemoglobin, collagen-associated fluorescence and little effect on regional albumin permeation [25]. It may prevent the formation of bis(lysyl)imidazolium protein cross-links formed from glyoxal, methylglyoxal, and 3-DG [1] and the putative cross-link 1,4-dideoxy-1-alkylamino-2,3-hexosulose formed by glucose-modified proteins [9], and prevent the formation of recognition factors for AGE receptors and concomitant vascular cell dysfunction [45]. A compound of the AG-type may eventually prove effective in the prevention of chronic pathology associated with diabetes and other AGE-associated disorders.

P.J.T. thanks the Medical Research Council (U.K.) for support for the research programme.

References

1. Thornalley PJ, Clinical significance of glycation. *Clin Lab* **5–6:** 263–273, 1999.
2. McCance DR, Dyer DG, Dunn JA, Bailie KE, Thorpe SR, Baynes JW and Lyons TJ, Maillard reaction products and their relation to complications in insulin-dependent diabetes mellitus. *J Clin Invest* **91:** 2470–2478, 1993.
3. Lyons TJ, Silvestri G, Dunn JA, Dyer DG and Baynes JW, Role of glycation in modification of lens crystallins in diabetic and nondiabetic senile cataracts. *Diabetes* **40:** 1010–1015, 1991.

4. Vitek MP, Bhattyacharya K, Glendening JM, Stopa E, Vlassara H, Bucala R, Manogue K and Cerami A, Advanced glycation end products contribute to amyloidosis in Alzheimer disease. *Proc Natl Acad Sci USA* **91:** 4766–4770, 1994.
5. Miyata T, Oda O, Inagi R, Lida Y, Araki N, Yamada N, Horiuchi S, Taniguchi N and Maeda K, β_2-Microglobulin modified with advanced glycation end products is a major component of haemodialysis-associated amyloidosis. *J Clin Invest* **92:** 1242–1252, 1993.
6. Vlassara H, Fuh H, Makita Z, Krungkrai S, Cerami A and Bucala R, Exogenous advanced glycosylation end products induce complex vascular dysfunction in normal animals: A model for diabetic and aging complications. *Proc Natl Acad Sci U S A* **89:** 12043–12047, 1992.
7. Lo TW, Selwood T and Thornalley PJ, Reaction of methylglyoxal with aminoguanidine under physiological conditions and prevention of methylglyoxal binding to plasma proteins. *Biochem Pharmacol* **48:** 1865–1870, 1994.
8. Hirsch J, Petrakova E and Feather MS, The reaction of some dicarbonyl sugars with aminoguanidine. *Carbohydr Res* **232:** 125–130, 1992.
9. Chen H-JC and Cerami A, Mechanism of inhibition of advanced glycosylation by aminoguanidine *in vitro*. *J Carbohydr Chem* **12:** 731–742, 1993.
10. Soulis T, Thallas V, Toussef S, Gilbert RE, McWilliam BG, Murray-McIntosh RP and Cooper ME, Advanced glycation end products and their receptors co-localise in rat organs susceptible to diabetic vascular injury. *Diabetologia* **40:** 619–628, 1997.
11. Hammes HP, Martin S, Federlin K, Geisen K and Brownlee M, Aminoguanidine treatment inhibits the development of experimental diabetic retinopathy. *Proc Natl Acad Sci U S A* **88:** 11555–11558, 1991.
12. Araki A, Glomb MA, Takahashi M and Monnier VM, Determination of dicarbonyl compounds as aminotriazines during the Maillard reaction and *in vivo* detection in aminoguanidine-treated rats. In: *The Maillard Reaction in Foods and Medicine* (Eds. O'Brien J, Nursten HE, Crabbe MJ and Ames JM), p. 400. RSC Publ., Cambridge, U.K., 1998.
13. McLellan AC and Thornalley PJ, Synthesis and chromatography of 1,2-diamino-4,5-dimethoxybenzene, 6,7-dimethoxy-2-methylquinoxaline and 6,7-dimethoxy-2,3-dimethylquinoxaline for use in a liquid chromatographic fluorimetric assay of methylglyoxal. *Anal Chim Acta* **263:** 137–142, 1992.
14. Madson MA and Feather MS, An improved preparation of 3-deoxy-D-*erythro*-hexos-2-ulose via the bis(benzoylhydrazone) and some related constitutional studies. *Carbohydr Res* **94:** 183–191, 1981.
15. Mendes P, GEPASI A software package for modelling the dynamics, steady states and control of biochemical and other systems. *Comput Appl Biosci* **9:** 563–571, 1993.
16. Daunis J, Jacquier R and Viallefont P, Etude en serie astriazine. IV. Syntheses de triazine-1,2,4 substituees en position 3. *Bull Soc Chim Fr* **10:** 3675–3678, 1969.
17. Baiocchi F, Cheng CC, Haggerty WJ Jr, Lewis LL, Liao TK, Nyberg WH, O'Brien DE and Podrebarac EG, Studies on methylglyoxal bis(guanylhydrazone) analogs. II. Structural variations on methylglyoxal bis(guanylhydrazone). *J Med Chem* **6:** 431–435, 1963.
18. Rae C, Berners-Price SJ, Bulliman BT and Kuchel PW, Kinetic analysis of the human erythrocyte glyoxalase system using ^{1}NMR and a computer model. *Eur J Biochem* **193:** 83–90, 1990.
19. Creighton DJ, Migliorini M, Pourmotabbed T and Guha MK, Optimisation of efficiency in the glyoxalase pathway. *Biochemistry* **27:** 7376–7384, 1988.
20. Betterton E and Hoffmann M, Henry's law constants of some environmentally important aldehydes. *Environm Sci Technol* **22:** 1415–1418, 1988.
21. Whipple EB, The structure of glyoxal in water. *J Am Chem Soc* **92:** 7183–7186, 1970.
22. Weenen H and Tjan SB, Analysis, structure, and reactivity of 3-deoxyglucosone. *ACS Symp Ser* **490:** 217–231, 1992.
23. Edwards AS and Wedzicha BL, Kinetics and mechanism of the reaction between 3-deoxyglucosone and thiols. *Food Addit Contam* **9:** 461–469, 1992.
24. Lo TW, Westwood ME, McLellan AC, Selwood T and Thornalley PJ, Binding and modification of proteins by methylglyoxal under physiological conditions. A kinetic and mechanistic study with N_α-acetylarginine, N_α-acetylcysteine, N_α-acetyl-lysine, and bovine serum albumin. *J Biol Chem* **269:** 32299–32305, 1994.
25. Nyengaard JR, Chang K, Berhorst S, Reiser KM, Williamson JR and Tilton RG, Discordant effect of guanidines on renal structure and function and on regional vascular dysfunction and collagen changes in diabetic rats. *Diabetes* **46:** 94–106, 1997.
26. Thornalley PJ, The glyoxalase system in health and disease. *Mol Aspects Med* **14:** 287–371, 1993.
27. Chibber R, Molinatti GM, Wong JS, Mirlees D and Kohner EM, The effect of aminoguanidine and tolrestat on glucose toxicity in bovine retinal capillary pericytes. *Diabetes* **43:** 758–763, 1994.
28. Bucala R, Makita Z, Koschinsky T, Cerami A and Vlassara H, Lipid advanced glycosylation: Pathway for lipid oxidation *in vivo*. *Proc Natl Acad Sci USA* **90:** 6434–6438, 1993.
29. Patthy L, Role of nascent α-ketoaldehyde in substrate-dependent oxidative inactivation of aldolase. *Eur J Biochem* **88:** 181–196, 1978.
30. Lal S, Kappler F, Walker M, Orchard TJ, Beisswenger PJ, Szwergold BS and Brown TR, Quantitation of 3-deoxyglucosone levels in human plasma. *Arch Biochem Biophys* **342:** 254–260, 1997.
31. Beisswenger PJ, Howell S, Touchette A, Lal S and Szwergold BS, Metformin reduces systemic methylglyoxal levels in type 2 diabetes. *Diabetes* **48:** 198–202, 1999.
32. Thornalley PJ and Minhas HS, Rapid hydrolysis and slow α,β-dicarbonyl cleavage of an agent proposed to cleave glucose-derived protein cross-links. *Biochem Pharmacol* **57:** 303–307, 1999.
33. Thornalley PJ, Modification of the glyoxalase system in human red blood cells by glucose *in vitro*. *Biochem J* **254:** 751–755, 1988.
34. Abordo EA, Minhas HS and Thornalley PJ, Accumulation of α-oxoaldehydes during oxidative stress: A role in cytotoxicity. *Biochem Pharmacol* **58:** 641–648, 1999.
35. Westwood ME and Thornalley PJ, Glycation and advanced glycation endproducts. In: *The Glycation Hypothesis of Atherosclerosis* (Ed. Colaco C), pp. 57–88. Landes Bioscience, Austin, 1997.
36. Corbett JA, Tilton RG, Chang K, Hasan KS, Ido Y, Wang JL, Sweetland MA, Lancaster JR Jr, Williamson JR and McDaniel ML, Aminoguanidine, a novel inhibitor of nitric oxide formation, prevents diabetic vascular dysfunction. *Diabetes* **41:** 552–556, 1992.
37. Al-Abed Y and Bucala R, Efficient scavenging of fatty acid oxidation products by aminoguanidine. *Chem Res Toxicol* **10:** 875–879, 1997.
38. Giardino I, Fard AK, Hatchell DL and Brownlee M, Aminoguanidine inhibits reactive oxygen species formation, lipid peroxidation, and oxidant-induced apoptosis. *Diabetes* **47:** 1114–1120, 1998.
39. Kang Y, Edwards LG and Thornalley PJ, Effect of methylglyoxal on human leukaemia 60 cell growth: Modification of DNA G_1 growth arrest and induction of apoptosis. *Leuk Res* **20:** 397–405, 1996.

40. Okado A, Kawasaki Y, Hasuike Y, Takahashi M, Teshima T, Fujii J and Taniguchi N, Induction of apoptotic cell death by methylglyoxal and 3-deoxyglucosone in macrophage-derived cell lines. *Biochem Biophys Res Commun* **225:** 219–224, 1996.
41. Hammes HP, Strodter D, Weiss A, Bretzel RG, Federlin K and Brownlee M, Secondary intervention with aminoguanidine retards the progression of diabetic retinopathy in the rat model. *Diabetologia* **38:** 656–660, 1995.
42. Cameron NE, Cotter MA, Dines K and Love A, Effects of aminoguanidine on peripheral nerve function and polyol pathway metabolites in streptozotocin-diabetic rats. *Diabetologia* **35:** 946–950, 1992.
43. Sugimoto K and Yagihashi S, Effects of aminoguanidine on structural alterations of microvessels in peripheral nerve of streptozotocin diabetic rats. *Microvasc Res* **53:** 105–112, 1997.
44. Soulis-Liparota T, Cooper M, Papazoglou D, Clarke B and Jerums G, Retardation by aminoguanidine of development of albuminuria, mesangial expansion, and tissue fluorescence in streptozotocin-induced diabetic rat. *Diabetes* **40:** 1328–1334, 1991.
45. Thornalley PJ, Cell activation by glycated proteins. AGE receptors, receptor recognition factors and functional classification of AGEs. *Cell Mol Biol* (Noisy-le-grand) **44:** 1013–1023, 1998.